

# Radargrammetric SAR image processing

Stéphane Méric, Franck Fayard and Éric Pottier  
*Institute of Electronics and Telecommunications of Rennes,  
European University of Brittany  
France*

## 1. Introduction

Throughout history, humans have tried to represent what they see through images. Mapmakers have always sought ways in which to represent both the location and the three dimensional shape of land. At the beginning, the way to obtain a 3D representation of land was to measure planimetry and height (as we can identify later by longitude, latitude and height) using basic measuring devices. Nowadays, the improvements of airborne and spatial instruments make it possible to produce images by sensing the electromagnetic radiation from the Earth. So, we can distinguish two classes of remote sensors: optical sensors and radar sensors. Optical sensors, such as Landsat or SPOT 5, operate around the visible spectrum and provide images with a fine resolution (less than 5 meters for SPOT 5). Thus, these kinds of sensors become very useful for civilian applications (cartography, elevation map, agriculture, hydrography, management of natural hazards, meteorology, geology, deforestation and so on). Considering the subject of this chapter, the extraction of terrain elevation by stereoscopic images can give digital elevation models with an error of about 5 meters (Toutin, 2000). However, optical sensors could be critically useless because of weather conditions or lack of light (i.e. sun). Thus, the use of radar sensors is a good way to overcome the limitations of optical sensors: not very sensitive to rain, considered as active sensors (because they have their own source of energy). Thanks to the signal processing applied to radar signal (pulse compression and synthetic aperture), radar systems can provide images with a very high resolution (for example, Radarsat-2 has an ultra-high resolution mode of about 3 meters for resolution). So, radar images are considered as additional information to optical images. With regard to these properties, one can estimate that radar images are used to get elevation terrain. The more intuitive way to extract depth information from remote sensing images is stereogrammetry. As the brain operates on optical images from eyes, the technique of radargrammetry is applied to SAR (Synthetic Aperture Radar) stereo data and provides digital elevation models (DEM). Considering this preamble to the radargrammetric world, this chapter examines one way to produce digital elevation models (DEM) from a mountainous area (the French Alps) and the way to improve the accuracy of the DEM. So, we will organize the discussion in three parts. In part 1, in order to better understand the stereo computation, we need to explain the basic characteristics of a radar image, which is particularly important to be considered during the radargrammetric processing. Thus, a radar image can be seen as a distribution of reflected electromagnetic energy on the ground. So, each element (i.e. a pixel) of an image is described by its size along the azimuth and range axis. Also, specific characteristics of a radar image are described as layover, shadowing and foreshortening. Because radargrammetric processing is

based on fitting images, we need to establish a common reference to radar images and to set up geographical coordinates for each image. Considering the position of the sensor, we can establish rigorous radar projection equations that can be compared to the so-called photogrammetric equations. As the radiometry is important to interpret a radar image, we consider the main radiometric models and the speckle phenomenon considered as noise in the SAR image. In part 2, considering a radar image, we will present the basic operations of extraction from satellite radar data. There are several methods to reconstruct elevation model from radar images. These images are essentially described as 2D information. So, one has to extrapolate 3D information from 2D description (as DEM). There are different methods to do this: clinometry, stereoscopy, interferometry and polarimetry. Since any sensor, system or method has its own advantages and disadvantages, the choice of a radargrammetric technique depends on the sensors and the means used during image acquisition. For the stereoscopic method, the capability of radar image pairing to achieve radargrammetric processing depends on geometric configuration in relation with the radar trajectory. Considering this radar trajectory, one can define the radar stereo base, the intersection angle and the parallax. We propose to review different ways to process the matching operations. These ways are correlation operations based upon searching for match points as area correlation methods or elementary correlation. After that, we will expose some improvements in the matching process (pyramidal scheme, speckle filtering). Part 3 will deal with the description of radargrammetric applications on real data (from SIRC shuttle mission) and the different steps to obtain a DEM. First of all, we describe the radar image and especially the relations between the satellite route and the ground radar image. This step is crucial in order to efficiently match the stereo radar images. Also, we explain the significance of using ground control points (GCPs) to rectify radar images. The next step is the matching operation between the two stereo SAR images. It consists in determining the point co-ordinates inside the secondary image for each point in the reference image, which is called the corresponding pixel. The computation of the 2D normalized cross-correlation coefficient is used on SAR images. At this step, we use a hierarchical strategy to reduce process time and use a filter to get the high accuracy disparity map. Then, we apply the rigorous radar stereo intersection problem and compute the stereo radargrammetric equations. Using the solutions, we obtain a DEM from the stereo radar images. This DEM is compared with a reference DEM. At the end, we move on to the point of improvement of the DEM: obvious improvements (correction of incoherent points) and further improvements in progress (use of adaptive correlation windows or polarimetric parameters).

## 2. Radargrammetric sensors

### 2.1 Introduction

As the acronym RADAR means "Radio Detection and Ranging", the basic principles are to detect and range objects located in front of the radar system. In the context of remote sensing, a scene (i.e. the terrain) is considered to be imaged by transmitting an incident electromagnetic wave from the radar, reflecting towards the radar (monostatic consideration) and receiving the reflected wave. The radar signal is obtained through the conversion of an electrical current on the antenna surface induced by an electromagnetic field around this antenna and vice-versa. Thus, the received signal contains information about the scene such as dielectric properties. Firstly, we can describe the received power  $P_r$  through the radar equation:

$$P_r = \frac{P_t \cdot G^2 \cdot \lambda_c^2}{(4\pi)^3 R^4} \sigma$$

where  $P_t$  is the transmitted power,  $G$  is the gain of the transmitted and received antenna,  $\lambda_c$  is the wavelength of the transmitted wave,  $R$  represents the distance between the radar and the scene and  $\sigma$  is the radar cross section. This parameter depends on many parameters such as the frequency and polarisation state of the emitted wave, the dielectric nature of the object, geometrical body of the object and so on. For example, buildings forming a corner with the ground or other buildings, correspond to high reflected energy. Conversely, roughness surfaces diffuse the incident energy and correspond to low reflected energy.

### 2.2 Signal processing and radar imaging

The side looking aperture radar (see figure 1) makes it possible to get radar images of the ground by emitting pulses of electromagnetic waves. The platform (aircraft or satellite) of

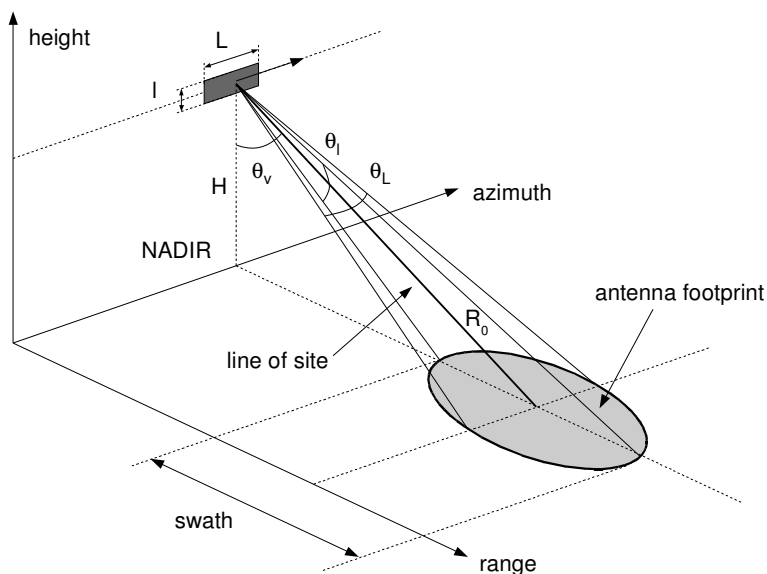


Fig. 1. Configuration of side-looking

such a radar travels forward in the flight direction or along-track (azimuth axis) with the nadir directly beneath the platform which is at the height  $H$ . The range axis refers to the across-track dimension perpendicular to the flight direction. The microwave beam is transmitted obliquely (elevation angle  $\theta_v$  to the direction of flight illuminating a swath. The side looking geometry is necessary to avoid the Doppler ambiguity. Some configurations exhibit a squint angle rather than an antenna pointing perpendicularly to the flight direction. The footprint of the antenna is defined through the line of sight of the main beam of the antenna and the aperture angles (along the range and azimuth axis) of this antenna. This aperture angle refers to the physical dimension of the antenna (respectively  $l$  and  $L$ ). Swath width refers to the strip of the Earth's surface from which data is collected by the radar. The longitudinal extent of the swath is defined by the motion of the aircraft with respect to the surface, whereas the swath width is measured perpendicularly to the longitudinal extent of the swath.

**2.2.1 Processing the image**

This chapter presents results from data obtained by a pulse radar. The word "resolution" means the precision to which we can measure the location of a point target and not necessary the capability of the radar to distinguish two targets (volume of confusion). Also, we can define the unfocused resolution along the range axis  $\delta_d = c\tau/2$  and along the azimuth axis  $\delta_a$  which partially depends on the value of  $R_0$ . At each position for the radar, an electromagnetic pulse is emitted with the period repetition commonly known as the inverse of the pulse repetition frequency (PRF). The pulse duration is very brief compared with the period of repetition. Thus, the reflected signal is recorded during almost the period repetition minus the pulse duration. The time of the beginning of the recorded signal is called  $t_p$  and the end is referred  $t_d$ . Also, we can define the physical limit of the radar image which is processed in the slant plane (see figure 2)

- the near range  $R_p = (c.t_p)/2$ ,
- the far range  $R_d = (c.t_d)/2$ .

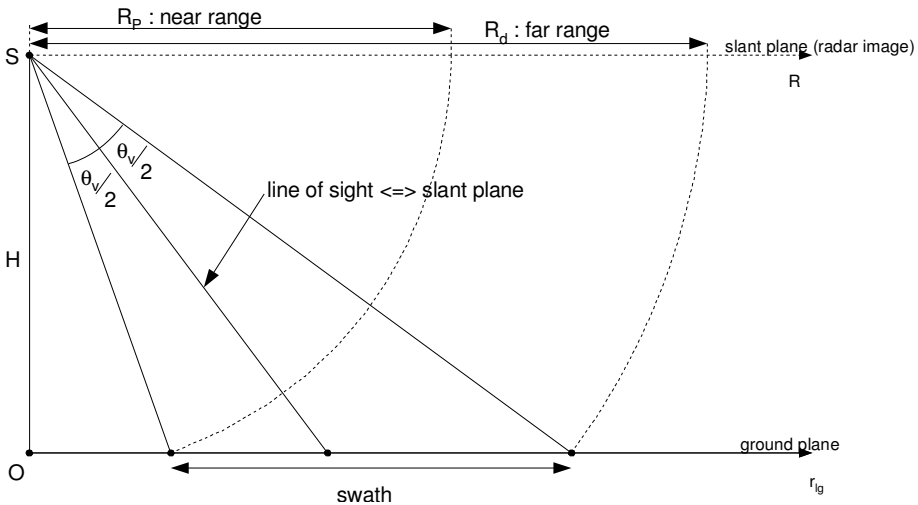


Fig. 2. Projection to the slant plane and to the ground plane

In order to get a ground-plane radar image, we have to interpolate and resample the slant-plane radar image and be sure that the range resolution is constant along the range axis. Ground-plane imagery must be obtained with minimal distortion if comparisons with maps taken from other sensors (for example sensors) are needed.

**2.2.2 Range resolution**

Actually, the term SAR refers to signal processing that improves the azimuth resolution. Considering the parameters of the SIR-C mission, the pulse duration is equal to  $33.8 \mu s$  and the resulting range resolution is more than 30 kilometers, which is unacceptable for remote sensing applications. Fine resolution is achieved by transmitting and receiving frequency modulated radar waves. The modulation is characterized by a wide bandwidth  $B_p$ . The echo is processed

by a matched filter that fine tunes the range resolution  $\delta_d$ :

$$\delta_d = \frac{c}{2.B_p}$$

Thus, the range resolution is inversely equal to the bandwidth of the emitted signal. Therefore, using the parameters of the SIR-C mission and especially the value of  $B_p$  (10 Mhz), we can get a range resolution of about 15 meters.

### 2.2.3 Azimuth resolution

Crossrange resolution is naturally achieved by use of an antenna with a narrow beam and specified by  $\theta_L$ . If the beamwidth along the crossrange axis is given approximately by  $\theta_L \approx \lambda/L$  where  $\lambda$  is the wavelength of the transmitted signal, the corresponding azimuth resolution  $\delta_a$  at range  $R_0$  is then  $\delta_a = \lambda.R_0/L$ . Considering the SIR-C mission again, the azimuth resolution would be about 30 kilometers, which is also unacceptable. The synthetic aperture processes the received signal by using the fact that the radar views the scene from slightly different angles. These different views (at each emitted pulse) are obtained because the radar moves through its synthetic aperture. Considering the response of one point on the ground, the reflected signal from this point can be seen as a frequency modulated signal (Doppler frequency). Also, a matched filtering operation is applied along the azimuth axis under certain assumptions (width of Doppler spectrum and duration of the seen point), we write the azimuth resolution  $\delta_a$  as

$$\delta_a = \frac{L}{2}$$

which gives an azimuth resolution of 6 meters considering the characteristics of the antenna of the shuttle (SIR-C).

### 2.2.4 Radar image corrections

The values of resolution given above are usually better than those obtained by the real system. Also, the signal processing must take into account undesirable effects that affect the performances of the radar. Concerning our discussion about radargrammetry, we can note among these effects:

- the range migration that can be modelled by the parabolic variation of the distance between the target point on the ground and the radar along the synthetic aperture (this point is corrected by different processing methods (Carrara et al., 1995)),
- the radiometric variations due to the change of received signal power from the beginning of the swath (near range) to the end of the swath (far range) for each position of the radar (using well-known ground points as RCS references can correct this effect),
- the motion compensation that corrects the deviation of the antenna from its nominal flight path.

Despite the corrections, some errors such as bad localization of pixels can still be found on the radar image. These errors can finally be eliminated by making use of ground control points such as buildings, cross-roads, mountain tops and so on.

**2.3 Geometric interpretation of a SAR image**

Actually, the importance of geometry for the interpretation of radar images recurs throughout this chapter. As we wrote before, the radar system can be considered as an ‘all-weather’ system and contrary to optical imagery, does not need ambient light or an external source of energy to obtain images. However, upon comparing a SAR image and an optical image, we can assume that certain properties of an optical image are not included in the radar image. For example, this phenomenon is clearly visible when looking at pixels farther from the radar, which appear smaller along the range axis than pixels closer to the radar. Although the cross range resolution is not affected by the radar imagery process, we suppose that the relief of the terrain will induce radiometric and, especially, geometric distortion. Thus, if we consider a ground point with a height  $h$  and located at a range  $R$  from the radar at the height  $H$ , the position  $x_{sol}$  along the range axis is given by:

$$x_{sol} = \sqrt{R^2 - (H - h)^2}$$

and means that a single radar image doesn’t give the altitude of a pixel but must be associated to a height model of the terrain. This is one of the tricky points about the interpretation of a radar image.

**2.3.1 Distortion of a radar image**

The projection of a terrain slope on the slant range of the radar induces well-known distortion that can be expected as regards the planimetry (see figure 3). And, the values of resolution

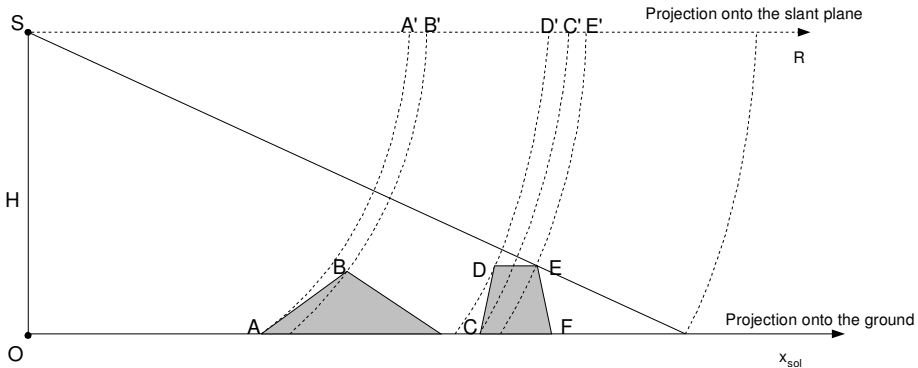


Fig. 3. Geometrical distortion occurs in the slant radar image.

given above are usually better than those obtained by the real system. Also, the signal processing must take into account undesirable effects that affect the performances of the radar. Concerning our discussion about radargrammetry, we can note among these effects the foreshortening effect, the layover effect and the shadowing effect which result from relief displacement.

**2.3.2 Foreshortening effect**

The foreshortening effect occurs when the radar beam reaches the base of a slope tilted towards the radar before the top of this same slope. The straight segment [AB] and its image [A'B'] onto the slant range illustrate this effect in figure 3. Thus, the radar measured distance

seems to be shorter than the real one and this effect is maximum when the radar beam is perpendicular to the mountain slope.

### 2.3.3 Layover effect

The layover effect occurs when the radar beam reaches the top of a mountain or a hill before its base. The straight segment [CD] and its image [C'D'] onto the slant range illustrate this effect in figure 3. Also, a terrain slope towards the radar produces a viewing permutation between the top and the base of a mountain on a radar image.

### 2.3.4 Shadowing effect

The shadowing effect occurs when the radar beam is not able to illuminate the radar scene. This effect that can be seen in figure 3 considering the straight segment from the point E', image of the point E, to the end of the swath. Also, the radar shadow is considered as an optical shadow and induces a black area on the radar image because no reflected wave comes from this kind of region (for example, point F is not seen on the radar image). All these effects are quite severe in order to understand a radar image well and especially in mountainous areas. Moreover, the incidence angle of the radar beam is another important parameter to estimate the influence on the interpreted radar image. So, the efficiency of the radargrammetric processing must take into account these characteristics.

### 2.3.5 Geometrical model of the radar position

The capabilities to link each pixel of a radar image to a real position on the terrain is one of the most important steps of the radargrammetric processing because correction, rectification, resizing and superimposition processings of the image need to know the geometrical position of a pixel. The model of the platform (e.g. in our study a satellite) flight path is described in figure 4 provides relation between radar image indexes and the terrain (Girard, 2003) thanks to

- radar parameters (frequency, size of the antenna, incidence angle ...),
- instantaneous position and motion of the radar platform,
- an ellipsoidal model of the Earth.

For the last item, the figure 4 gives several parameters to describe the model as

- angles  $\lambda$  and  $\phi$  which are respectively the longitude position and the latitude position,
- Earth's referential  $(G, i, j, k)$  which is established by the centre of the Earth G, the i-axis towards the Greenwich meridian, the k-axis coinciding with the Earth's axis of rotation and the j-axis forming a right-handed system with i-axis and k-axis instantaneous position and motion of the radar platform,
- referential of satellite  $(S, l, r, t)$  linked to the satellite and described by the position S of the satellite, the l-axis colinear to the vector  $\vec{GS}$ , the t-axis simultaneously perpendicular to the l-axis and the vector  $\vec{S}$  and the r-axis forming a right-handed system with l-axis and t-axis.

As described in (Dhond & Aggarwal, 1989), stereoscopic processing needs to know several parameters which corresponds, for radargrammetry processing, to:

- the wavelength  $\lambda_c$  of the transmitted wave,
- the azimuth resolution  $\delta_a$  and the range resolution  $\delta_d$ ,

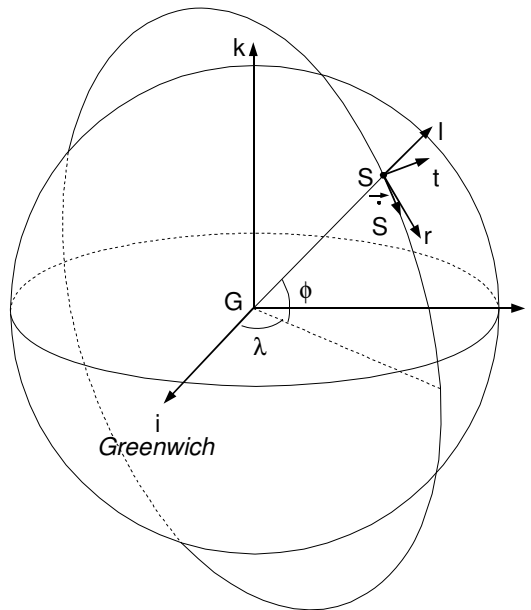


Fig. 4. Position and motion of a satellite

- the central Doppler frequency  $f_D$  of the received signal,
- the time  $t_0$  for which the values of the position and the velocity of the satellite are known,
- the initial time  $t_{init}$  of the beginning of the radar image,
- the range distance  $r_0$  given for a reference line of the image,
- parameters that make it possible to calculate the behaviour of the satellite (position, orientation, velocity) for each value of time.

Actually, the position and velocity of the satellite are known at specific values of time which are called ephemerides. Thus, we have to interpolate the path of the satellite in order to have all the position and velocity of the satellite along the flight path.

### 2.3.6 Geographic coordinates of a radar image

Thanks to the parameters describing the flight path of the satellite, it is possible to give geographic information for each pixel of the radar image. In order to establish this relation and to measure locations accurately, some references of coordinates are used (Dufour, 2001). In this chapter, we use the global coordinate system which has been described before (see figure 4). The ellipsoidal height  $h$  of a point is the vertical distance of the point in question above the reference ellipsoid. The reference ellipsoid is described by the WGS84 system (geodetic) and the significant parameters defined by

- the semi-major axis  $a = 6378137.0$  meters,
- the semi-minor axis  $b = 6356752.3$  meters.



Considering a point M defined by its height  $h$  and its geocentric coordinates  $(x, y, z)$  in the  $(G, i, j, k)$  reference, we can write the above expression:

$$\frac{x^2 + y^2}{(a + h)^2} + \frac{z^2}{(b + h)^2} = 1$$

**2.3.7 Radar coordinates and image coordinates**

In the radar reference, each pixel of the image gives information about the range distance  $r$  and the time  $t$  elapsed since the beginning of the recorded raw data. Another way to describe a radar image refers obviously to the azimuth  $u$  and range  $r$  coordinates. Also, a data transformation is feasible via the number of looks  $N_f$  used to establish the radar image (Curlander, 1991) and the spatial sampling frequency  $f_e$  along the range axis:

$$\begin{cases} t &= \frac{N_f}{f_r} \cdot u + t_{init} \\ r &= \frac{c}{2f_e} \cdot v + r_0 \end{cases}$$

We have to note that the values of  $u$  and  $v$  are immediately obtained from the radar image. At this time, we have to set up the coordinates  $t$  and  $r$  in the defined Earth’s reference.

**2.3.8 Range sphere and Doppler cone**

We can define the range sphere as the constant distance  $r$  of a point M from the radar located at the position S:

$$|\overrightarrow{SM}| = r$$

Moreover, the Doppler cone is the cone of equal Doppler frequency and has its apex located at the centre of the range sphere:

$$f_D = \frac{2}{\lambda_c} \cdot \frac{\vec{S} \cdot \overrightarrow{SM}}{|\overrightarrow{SM}|}$$

In the case of side-looking radar, the centroid Doppler frequency  $f_D$  is equal to zero, which means the cone becomes a plane perpendicular to the velocity vector  $\overrightarrow{SM}$ . Considering the coordinates

- $(x, y, z)$  of the point M on the radar image,
- $(X_S, Y_S, Z_S)$  of the position S of the radar,
- $(\dot{X}_S, \dot{Y}_S, \dot{Z}_S)$  of the velocity of the radar,

the equations 2.3.7 and 2.3.8 establish a system of 2 equations of 3 unknowns  $(x, y, z)$  whose solutions describe a circle called Doppler circle (see figure 5). The Earth’s model as defined before and raised of height  $h_e$  finally makes it possible to get two solutions of the given system. One of these can be eliminated considering the line of site (LOS) (figure 6). Unfortunately, the different slopes of terrain above the Earth’s ellipsoid that we described before and the associated effects (especially in foreshortening areas) on the radar image result in more than one solution.

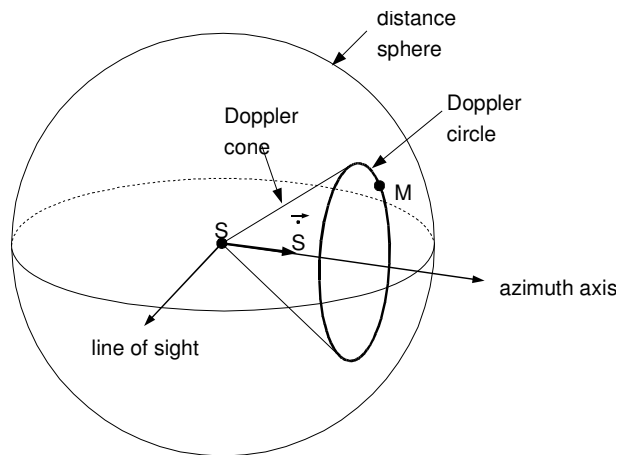


Fig. 5. Description of the distance sphere, Doppler cone and Doppler circle

#### 2.4 Radiometric phenomena in an SAR image

The first remark concerns the main difference between the radar image and the optical image. The Earth's surfaces reflecting strong energy towards the radar correspond to very bright pixels on the radar image (and can appear dark on an optical image). The radar scene reflects a certain amount of radiation according to its geometrical and physical characteristics. This part will deal with radiometric phenomena that occur on the ground and which essentially depend on the electrical properties of the soil and the roughness of the area. Moreover, as we have seen before, the geometric shape of an area or an object on the ground mainly determines the radiometry of a pixel and the brightness of a feature could be a combination with other objects. Another important parameter is the wavelength of the incident radiation wave and the electromagnetic interaction falls with either surface interaction or volume interaction. Also, we can separate the interactions into two main topics:

- smooth surfaces that reflect (nearly) all the incident waves towards to a particular direction: specular reflection. If the surface is tilted towards the radar, the corresponding radar image appears very bright. Conversely, if the surface is not turned towards the radar (e.g. calm water or paved roads), the surface appears dark on the radar image;
- rough surface that scatters the incident wave in many directions: diffuse reflector.

In order to determine the degree of roughness of a surface, we use to establish (Beckman & Spizzichino, 1987) a relation between the state of the surface quantified by the average height variation  $h$ , the wavelength of the wave  $\lambda_c$  and the local incidence angle  $\theta_i$  (see figure 7). This relation is known as the Rayleigh criterion:

$$\begin{cases} h < \frac{\lambda_c}{8 \cos \theta_i} \text{ lorsque } \lambda_c \gg h \\ h < \frac{\lambda_c}{32 \cos \theta_i} \text{ lorsque } \lambda_c \simeq h \end{cases}$$

Let us consider the local incidence angle: an incidence angle is the angle between the radar beam and the target object. The value of this angle determines the radar appearance of this

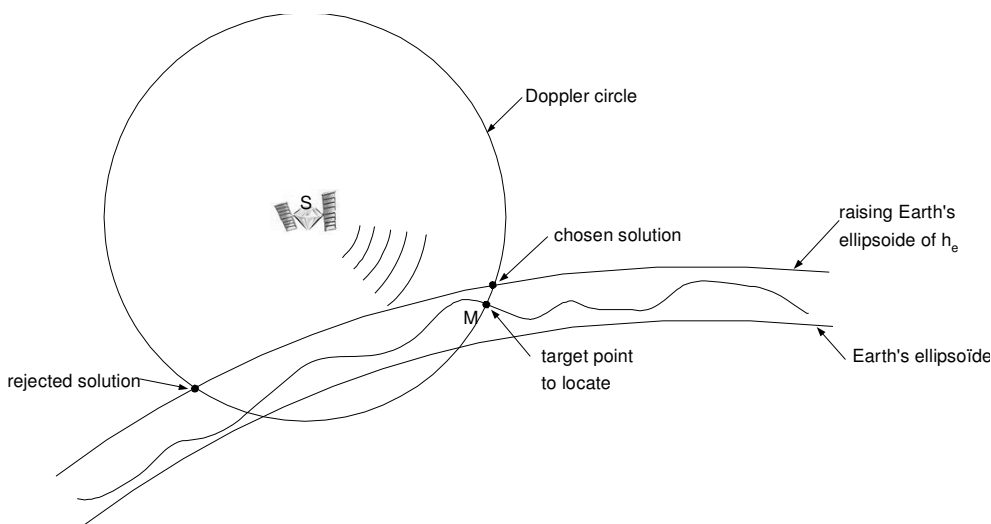


Fig. 6. Intersection of the Doppler circle and the Earth's surface

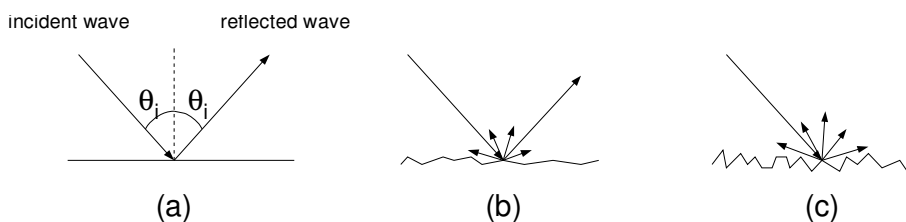


Fig. 7. Rayleigh criterion: (a) smooth surface, (b) low roughness surface and (c) high roughness surface

target on the radar image. Moreover, we can attach to each pixel of the radar image a local incidence angle so that we can notice variations in pixel brightness concerning one target object (rocks, trees, grass, buildings). Finally, we can note that the variation of incidence angles is less for a satellite radar than an airborne radar because of the height of the platform. Among the natural Earth's surfaces, we can characterize (Ulaby, 1981) three kinds of surface

- bare surface where simple reflections occur and the amount of energy towards the radar depends on the roughness of the soil,
- farmed surface where reflections are quite complex and depend on the crops, the moisture, the direction of the parcels and so on,
- vegetation surface where the reflection phenomena essentially depend on the wavelength. For example, the waves of the radar band X are only reflected by the top of the canopy. Lower wavelength waves penetrate the canopy and volume scattering has to be considered. Finally, some features on the ground can be considered as close targets, which means these features have two (or more) surfaces (generally smooth) forming a right angle and cause double (or more) bounce reflections (figure 8).

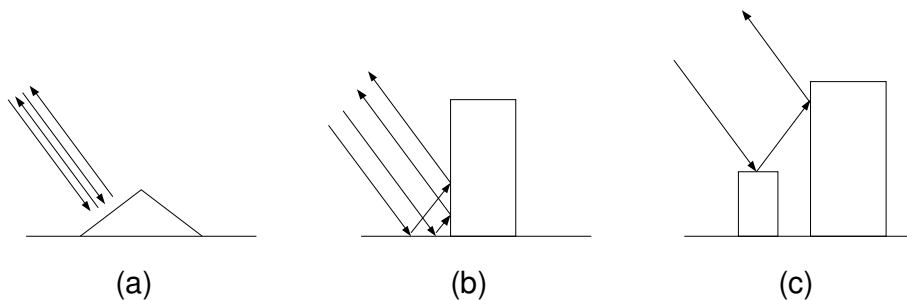


Fig. 8. Reflection phenomena: (a) from slope towards the radar, (b) from corner reflector (double bounce reflection) and (c) multiple bounce reflections.

The typical occurrence of this phenomenon is the corner reflection. Corner reflectors are very common in urban sites and show up as very bright targets on the radar image.

#### 2.4.1 Speckle phenomena

As the radar image is created through a radar coherent wave, a particular effect modifies the radiometry of pixels as a noise-like effect inherent in coherent imaging systems. This effect is obviously visible on large covered-grass areas and looks like a "salt and pepper" texture. This texture is due to the chaotic response of multiple small targets on the ground whose global response is seen as a constructive or destructive random process. Thus, this kind of process randomly produces bright and dark pixels: the radar image is speckled. Many articles are dedicated to the study of the speckle phenomena (Goodman, 1976). Even it could be considered as information for special applications, the speckle effect is seen as a multiplicative noise and degrades the quality of a radar image.

### 3. Radargrammetric operations

#### 3.1 State-of-the-art

The definition of radargrammetry has been stated by Leberl (Leberl, 1990): "Radargrammetry is the technology of extracting geometric information from radar images". To extract the geometrical characteristics of the ground, four different techniques are implemented: stereoscopy, clinometry (Horn, 1975), interferometry (Massonet & Rabaute, 1993) and polarimetry (Schuler et al., 1996). These are usually combined with SAR systems which have been briefly presented in this paper. Because the aim of this chapter is only to expose the radargrammetry as a radar stereoscopic method, the other ones will not be more developed. The first works on radargrammetry began after the Second World War and the first principles were defined by La Prade (La Prade, 1963). These works were completed by several mathematical developments (Gracie et al, 1970) and fully developed by numerous researchers (Rosenfeld, 1968) (Leberl, 1990) (Polidori, 1997). All of these developments were tested and improved thanks to several operational measurements both airborne (for example (Azevedo, 1971) mapping the world's tropical belt) and spatial (for example (Schrier, 1993) geocoding radar images from ERS-1 mission). Since the 1980s with the Shuttle Imaging Radar (SIR-A, SIR-B and especially SIR-C), the European satellite (ERS-2 and ENVISAT), the Canadian sensor (RADARSAT-1 and 2), the number of researchers working on the radargrammetric topic has increased and data

analysis has become more sophisticated (various incident angles, various frequencies and polarisations of the wave and so on).

### 3.2 Basics of radargrammetry as a radar stereoscopic method

#### 3.2.1 Principle

Stereoscopy is a viewing method that forces our eyes to see, at the same time, two images taken from different angles. This technique allows us to see in three dimensions as it reinforces physiological indicators. The indicators used by stereoscopic method are parallax and convergence angle and can be defined as follows:

- the parallax  $P$  of an observed point is a parameter that is directly connected to the point elevation and it increases with the altitude of the point,
- the convergence angle  $\Delta\theta_v$  is defined by the intersection of the two lines of sight of the radar and this angle increases as the baseline  $B_s$  rises.

In figure 9, the same-side stereoscopic configuration is exposed and the description of the parallax  $P$ , the base-line  $B_s$  and the intersection angle  $\Delta\theta_v = \theta_{v1} - \theta_{v2}$  is given. The latter parameters have an important function as regards the quality and the accuracy of the terrain reconstruction.

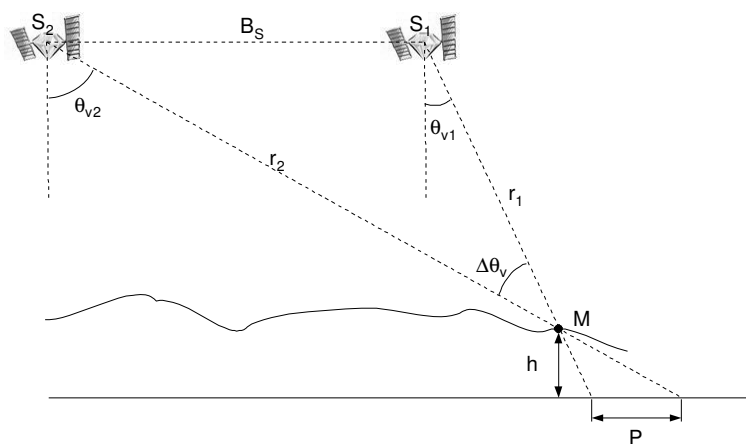


Fig. 9. One radar stereoscopic configuration.

#### 3.2.2 Matching step

Stereoscopic techniques applied to radars are influenced by optical techniques (we can compare the baseline  $B_s$  in the radargrammetry configuration and the vertex in the human description), except that SAR images replace optical systems images. But, the main difficulty is to get used to new and unnatural radar viewing (as we exposed before) and especially when both geometric and radiometric disparities are large. However, radar images can be viewed in stereo after training. The point of radargrammetry is to match two radar images by a "registration" processing. The registration step aligns two images containing the same radar scene but viewed from different positions. The aim of the matching step is to get a dense description in order to achieve the accuracy of image registration. The main difficulty of the registering

operations comes from the dissimilarities between the pair of images that are caused by different imaging configurations. The identification of corresponding image points is the main feature of the processing. This step is generally achieved by using several methods and we will present two of them:

- grey-level image matching,
- edge-based method.

The first one is generally computed with the normalised cross-correlation coefficient (Leberl et al., 1994) and many improvements such as the use of the sum of mean normalised absolute difference or the least squares solutions are investigated. The second one is based on the fact that an object or a structure may look quite similar in both images whatever the radar position (Marr & Hildreth, 1980). However, this method needs some preprocessing (e.g. filtering operations) in order to be really efficient and the application to, for example, a mountainous area is not possible because of the small area of edges relatively to the total area of images. Thus, the combination of both methods can achieve good results (Paillou & Gelautz, 1999).

### 3.2.3 Disparity measurement and terrain reconstruction

For each pair of images, we get one map of disparities along both the azimuth axis and the range axis. In the case of a flat Earth, no disparity along the azimuth axis should occur when radar images come from parallel flight paths. But, because of the lack of precision of the radar trajectories, azimuth disparities exist and the way to eliminate these is to resample images into an epipolar geometry. At the end of the radargrammetric processing, the computation of a disparity map obtained under the flight conditions produces the terrain elevation which is called DEM (e.g. Digital Elevation Model). The calculated height of each pixel on the image agrees with the different equations describing the geometry of the flights of path. Moreover, in order to get a better DEM, the use of ground control points is essential to correct the geometric model of the terrain and to set up the best stereomodel as regards the solution of the stereo geometry.

## 3.3 Radargrammetric processing

As the radargrammetric method was briefly described in the late section, we intend to expose more precisely all the steps required to reach a terrain elevation thanks to a pair of stereo radar images.

### 3.3.1 Acquisition of stereo images

An important radar stereoscopic issue is the way measurements have to be made. Two main configurations can be considered: same-side (the radar is located on the same side considering the position of the two radars) and opposite-side (the scene is located between the two radars) viewing. Considering the same-side configuration (see figure 10), a large baseline (e.g. a large intersection angle) makes it possible to achieve good geometry for stereo plotting because of the increase in parallax values. And the higher the parallax value is, the more accurate the elevation reconstruction is. Conversely, the matching processing needs to manipulate images as closely identical as possible in order to succeed in stereo viewing. That implies a small intersection angle. The opposite-side configuration (figure 11) provides a large baseline and thus precise stereo plotting. Moreover, we can see in figures 11 and 10 the consequence of a range estimation error (the real point  $M$  migrates to the point  $M_e$  that is located by processing) that is less significant in the opposite-side case than the same-side one. But, the radiometric differences are so important in the case of opposite-side configuration that the matching operation

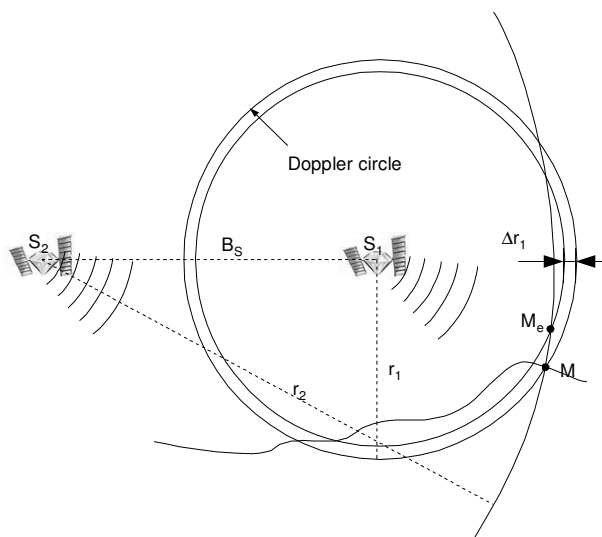


Fig. 10. Same-side configuration and range error consequence

is almost impossible without a preprocessing of images (for example, radiometric inversion). However, some studies (Toutin & Gray, 2000) demonstrate that we can have conflicting conclusions about theory developments and image applications. Anyway, the choice of the pairs of stereoscopic images comes up regarding the capability to get the parallax values and the accuracy of the height reconstruction. Thus, a compromise has to be reached between these two topics and concerns the baseline  $B_s$  to the height  $H$  of the platform ratio. This ratio can vary from 0.25 to 2. For example, a study about RADARSAT measurements (Sylvander et al., 1997) suggests an intersection angle of about  $8^\circ$  that corresponds to a value of  $B$  on  $H$  ratio equal about 0.3.

**3.3.2 Correlation matching operation**

The most common image matching method is area correlation. For a given area in the primary image, the matching computation has to detect the closest one in the secondary image by searching for the best matched area. The difference of position is the value of the parallax or disparity. The classical method of finding match areas is to use an analytical metric comparison and the zero-mean normalized cross-correlation (ZNCC) can be applied to searching for windows of radar images. These windows are usually squared and the size is  $(2n+1)$  by  $(2n+1)$  pixels, so a centre pixel can be defined. The ZNCC is often used because of robustness on the radiometric variations of the radar image and the result is given by the cross-correlation coefficient  $\rho$ . This coefficient  $\rho$  can be stated as follows:

$$\rho = \frac{E[I_1 I_2] - E[I_1]E[I_2]}{\sqrt{V(I_1)V(I_2)}}$$

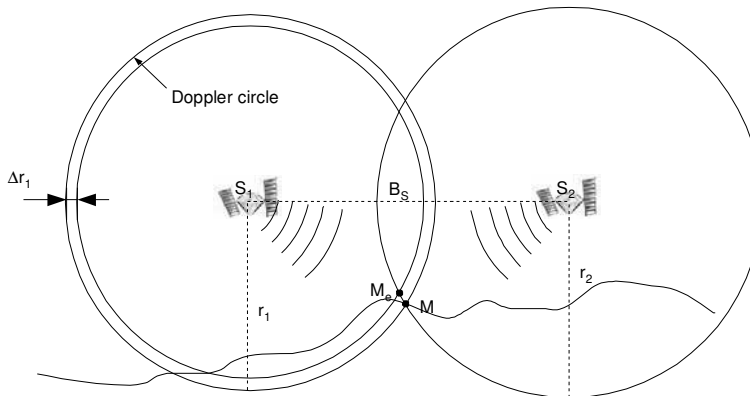


Fig. 11. Opposite-side configuration and range error consequence

where  $I_1$  and  $I_2$  represents the amplitude value of the pixels of the window. The mean or mathematical expectation  $E[I_i]$  is calculated thanks the following expression:

$$E[I_{1,2}] = \frac{1}{N} \sum_{k=1}^N I_{1,2}^k \quad (1)$$

where  $N$  represents the number of pixels inside the window. Moreover, the variance expression  $V(\cdot)$  about the window  $I_i$  is given by:

$$V(I_{1,2}) = E[(I_{1,2} - E[I_{1,2}])^2] \quad (2)$$

The value of  $\rho$  is bounded by (-1) and (+1) and the windows are considered matched for the maximum value of  $\rho$ . The coefficient  $\rho$  is calculated for each position ( $az_s$  and  $rg_s$ ) of the researching window in the researching area. Also, we get a correlation surface obtained with the values of the coefficient  $\rho$  and the maximum of this surface gives the disparity  $disp_{az}$  along the azimuth axis

$$disp_{az} = |az_s(\max) - az_r|$$

and the disparity  $disp_{rg}$  along the range axis

$$disp_{rg} = |rg_s(\max) - rg_r|.$$

This step is carried out for each point of the primary image in order to get the disparity map. The figure 12 illustrates the correlation computation applied for one pixel inside the primary image. Considering the assumptions of radiometric distortions in a radar image, the cross-correlation computation does not work very well on such degraded images (shadowing effect for example). That is the reason why the choices of the viewing configuration and the value of  $B_s$  are very important. Especially in mountainous areas, a large part of unmatched pixels can occur because of the shortening and layover effects. Finally, the choice of the greatest value of  $\rho$  for a given correlation computation is not necessarily the optimum criterion but must be considered with other parameters. Several methods can be applied to improve the matching operation.



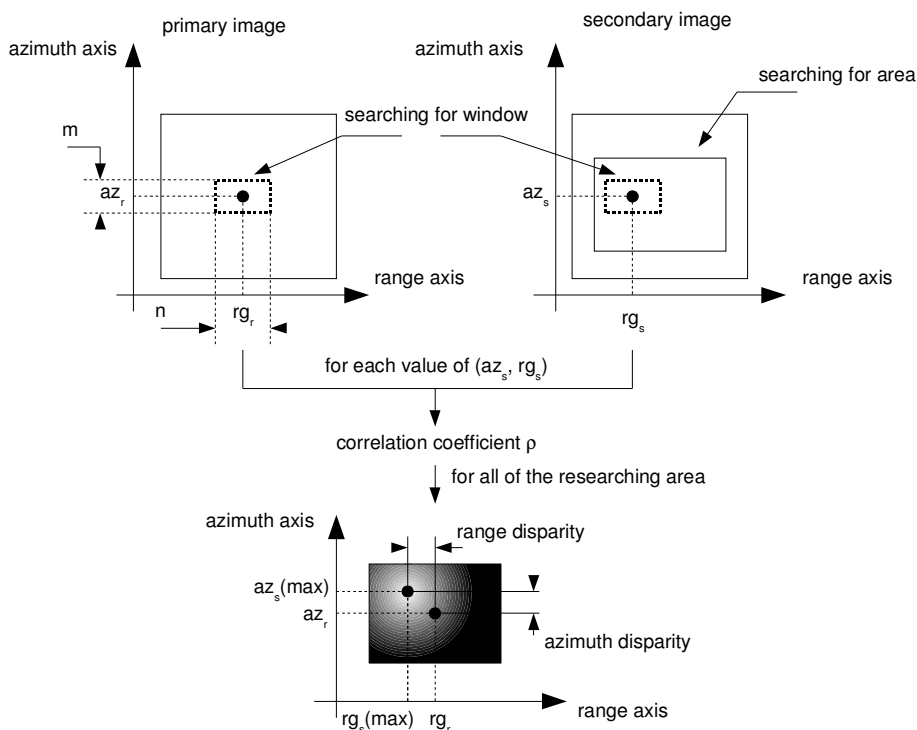


Fig. 12. Matching operations between primary image and secondary image.

### 3.3.3 Epipolar geometry

The use of smaller correlation windows is one way to limit the false matching result. For example, an epipolar constraint (Zhang et al., 1995) can be applied and reduce the research of the matched window along the azimuth axis. Considering parallel flight paths at a constant altitude and using the epipolar geometry, we can reduce the search area assuming that for a given point in an image, the corresponding point is located on the same azimuth line. Ideally, the search area can be reduced on a thin strip of one pixel thickness on the epipolar line. Practically, it is better to have a reduced search area one to 3 pixels wide along the azimuth axis because the estimation errors can lead to mistaken parameters. Finally, the epipolar geometry considerably reduces the size of the search area and also reduces computing time. Moreover, it limits false matching because for one pixel to match, there are fewer candidates on the other images than a larger window. The second way uses a partial knowledge of the terrain elevation that limits the research along the range axis: knowing the minimum and maximum elevation of the area, we compute the minimum and the maximum disparities along the range axis.

### 3.3.4 Pyramidal procedure

Another way can be considered as a hierarchical strategy used to reduce processing time and to make it possible to work with large images (Denos, 1992). The principle is quite simple:

## Thank You for previewing this eBook

You can read the full version of this eBook in different formats:

- HTML (Free /Available to everyone)
- PDF / TXT (Available to V.I.P. members. Free Standard members can access up to 5 PDF/TXT eBooks per month each month)
- Epub & Mobipocket (Exclusive to V.I.P. members)

To download this full book, simply select the format you desire below

